Thermal Analysis of AlGaN/GaN HEMT: Measurement and Analytical Modeling Techniques

Balwant Raj
Punjab University Chandigarh
Dept. of ECE,
PU Regional Centre Hoshiarpur

Sukhleen Bindra, Ph.D
Professor, Dept. of Electronics Engineering
GNDU, Amritsar
Punjab, India

ABSTRACT

In this paper, the temperature dependent electrical measurements by employing a Quantum Focus Instrument (QFI) and analytical analysis were presented and applied to Aluminum Gallium Nitride, Gallium Nitride (AlGaN-GaN) High Electron-Mobility Transistors (HEMTs). The analytical evaluation of band bap energy, electron mobility, thermal conductivity and thermal resistance has been carried out. The electrical measurements have been done using network analyzer with infrared IR measurement technology. The results obtained on the basis of electrical measurements are compared with analytical and simulated results for the purpose of validation of our outcomes. The measured data shows a good agreement with analytical and simulated results, thereby validating our approach of AlGaN/GaN HEMT analysis.

Keywords

Thermal Simulations, AlGaN/GaN, HEMT, Modeling, Measurements,

1. INTRODUCTION

The emergent GaN HEMTs (High Electron Mobility Transistor) is important due to its superior material properties such as high breakdown voltage with high cutoff frequency compared to the other material based devices, leading to high power and high efficiency amplifiers for next generation wireless communication, satellite communication and radar systems. Famous abilities have been demonstrated by several papers [1, 2]. The capability of generating high RF output power makes AlGaN/GaN HEMTs an appealing alternative to traditional GaAs and InP devices [3]. The AlGaN/GaN-based HEMTs have been recognized as the most promising devices for high-power applications at microwave and millimeter-wave frequency range. However, the power performance of the AlGaN/GaN-based devices has been limited by surface trap-induced current dispersion phenomenon, which reduces the RF current swing and increases the RF knee voltage under large-signal operation.

As with all semiconductor devices, GaN HEMT device reliabilities are dependent directly on maximum operating channel temperature [4]. It is therefore important to determine, with a high degree of confidence, what the maximum channel temperature is under specific operating modes, and dissipating large amounts of thermal energy. In addition to understanding the maximum channel temperature of a device for reliability, it is equally as important to understand thermal resistance of packaged transistors for system level design [5].

Proper thermal management is critical for GaN-based HEMT devices because localized self-heating effects under high-power, high-frequency operation significantly impact device performance and reliability. Since heat generation is concentrated within a small volume at the drain-side edge of the gate contact [6], measurement of the temperature in the active region of the device requires high spatial resolution. For multi-finger devices, the boundary conditions are different for each channel resulting in a complex, nonuniform, 3-D temperature distribution across the device. Simple thermal models commonly used assume that heat is generated at the gate contact or from a limited region on the drain-side edge of the gate. More accurate, full electrothermal models have been developed [6] to simulate the thermal profile of AlGaN/GaN HEMT devices under operating conditions, and these device simulations can reproduce the I_d-V_d characteristics observed experimentally. However, time-to-failure predictions based on accelerated lifetime testing require accurate thermal profiles both at the point-of-failure and under normal operating conditions, because extrapolation of these data over several decades in time make the predictions extremely sensitive to small errors in temperature [7]. Several experimental probes are commonly used to measure temperature profiles of biased HEMT devices, such as IR thermal imaging [8], as well as μ-Raman [9] and μ-PL [10] spectroscopies. Each of these techniques has its own unique advantages and disadvantages for this purpose, and they each provide limited spatial information.

This paper presents improved AlGaN/GaN HEMT model, which takes into account the self heating effect that appears mostly in high power GaN HEMTs. In this work carried out analytical modeling of band gap energy, thermal conductivity, mobility model, thermal resistance measurement and simulation of AlGaN/GaN HEMT. It has opened the door to new possibilities for high speed, high power and large current-handling capability. The subsequence section of the paper is organized as: Section 2 HEMT device structure under study. In Section 3 thermal measurement and experiment detail are described. Section 4 presents the AlGAN/GaN HEMT thermal analysis and effect of temperature variation on the performance metrics. In section 5 AlGAN/GaN HEMT analytical modeling discussed. In section 6 results and discussion are explained. In Section 7 conclusions are drawn.

2. HEMT DEVICE STRUCTURE UNDER STUDY

The device AlGaN/GaN HEMT is shown in figure 1.a and schematic draw of AlGaN/GaN HEMT device is shown in figure 1.b. The basic geometrical parameters of the HEMT are the gate length L_g and the gate width W_g (see figure 1.b).

Other characteristic dimensions are the thickness of active layer respective distance of the gate contact from conductive channel d, the gate to source and the gate to drain terminal spacing, L_{gs} and L_{gd}. Dimension L_g is critical in determining the maximal frequency limits for the device. The drain current flowing through the device is directly proportional to the gate width W_d [18]. Therefore for low noise, low current application relatively small-gate-width devices are utilized, in contrast to large-gate-width devices used rather in power applications.

Because of the strong spontaneous and piezoelectric polarization of GaN and its ternary, a high density two dimensional electron gas (2DEG) is induced at the heterojunction interface and confined in the triangular potential well due to the large band discontinuity. The high electron velocity, which is estimated above 10^7 cm/s, bodes well for high frequency operation, and the large breakdown voltage allows for high power applications to be exploited.

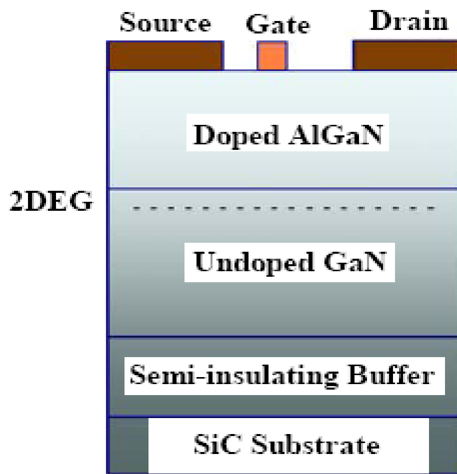

Figure 1.a AlGaN/GaN HEMT Structure

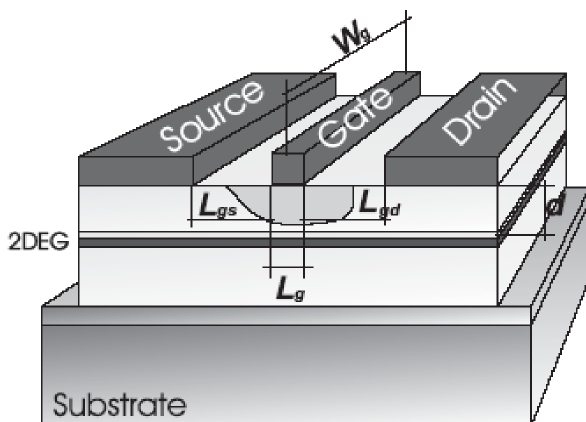

Figure 1.b Schematic draw of AlGaN/GaN HEMT device.

The band diagrams of the AlGaN/GaN HEMT device, with triangular potential well is shown in figure 2.a. Upon applying of a positive voltage to the drain, current transport along 2DEG will start, because of potential drop between source and drain. The magnitude of the current is controlled by the applied voltage to gate contact V_G. Increasing gate voltage into the negative values forces the space charge below the gate to spread towards two dimensional channel with electrons. After reaching the channel this starts to deplete under the gate region and so affects the drain current, until the channel is pinched-off see figure 2.b. By gate voltage above pinch-off electrons flow between source and drain. With increasing the drain bias, the drain-source current increases linearly up to certain value. After this value the current through the channel starts to saturate. The maximal saturation value I_{DSS} depends on the concentration of 2DEG. With increasing 2DEG concentration I_{DSS} increases what correspond to the amount of particles able to transfer the charge in the channel [19]. The dependence of the drain-source current (I_D) on applied voltage (V_{DS}) is depicted in figure 4.

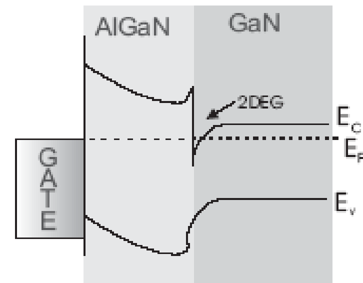

Figure 2.a Band Diagram of AlGaN/GaN HEMT at zero gate voltage.

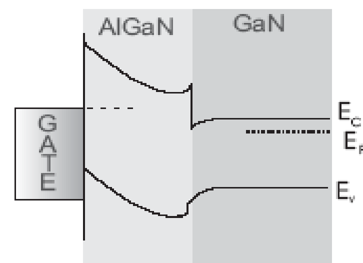

Figure 2.b Band Diagram of AlGaN/GaN HEMT at negative gate voltage

AlGaN/GaN HEMTs are the focus of attention in wireless communication and power electronics applications for high frequency, high temperature and high power performance. After much advancement and commercialization in GaAs-based devices, AlGaN/GaN-based HEMTs are getting increasing demand due to their higher bandgap and greater temperature handling capacity. Large polarization constants of these materials induce a high density of 2D electron gas (2DEG) 5-10 times greater than that in other III-V material [11, 12]. This is true even in undoped structures where the 2DEG is induced entirely from polarization effects, which further increases carrier mobility since no impurity scattering will be present. This characteristic leads to high speed, high power, and low noise performance in high temperature operation.

3. THERMAL MEASUREMENT AND EXPERIMENTAL DETAIL:

3.1 Measurement Technique:

The thermal analysis of HEMT structures for Monolithic Microwave Integrated Circuits (MMICs) is important, due to

increased circuit packing densities and RF output powers. We used the IR measurement technology necessary to obtain accurate temperature profiles on the surface of HEMT devices. The results will show how the measurement technique has been applied to study the thermal performance of GaN HEMT. Thermal modelling used to predict the junction temperature of individual HEMT device. Thermal models are not always accurate, as thermal constants, for example, the thermal boundary resistance, are often unknown. Experimental temperature measurements are therefore necessary for both specifying difficult parameters and model validation. In this work we used Infrared thermal microscopy technique, enabling non-invasive 2-D surface temperature measurements to be rapidly made on microwave devices, in both wafer and package forms. An IR thermal microscope facility has been established, employing a Quantum Focus Instrument (QFI) with state of the art spatial resolution of around 2.5 μm in the 2 - 5 μm wavelength bands.

Temperature measurement with electrical techniques exploits an electrical temperature sensitive parameter of a device. For example, the forward voltage of a Schottky junction as found in a High Electron Mobility Transistor (HEMT). If this temperature dependence is understood, electrical measurements can be used to establish the junction temperature [20]. A limitation with electrical techniques is they can only be used to give a single average junction temperature and cannot be used to detect hotspots or generate two dimensional temperature maps across structures with multiple heat sources, such as on MMICs. Temperature measurements can also be made using Atomic Force Microscopy (AFM), which employs a scanning thermal probe to enable two-dimensional mapping. Measurements made using AFM have achieved sub micrometer resolutions [21], although surface topology can give rise to some measurement error. For large area two-dimensional surface temperature mapping, IR thermal microscopy can be used [22]. Infrared thermal microscopy is a non-contact technique, utilizing naturally emitted infrared radiation from a sample, resulting in a real time thermal image. Infrared thermal microscopy involves the measurement of naturally emitted infrared radiation from the surface of a semiconductor device, such as an MMIC. Materials on the surface of the semiconductor device can vary in ability to emit infrared radiation. A ratio known as 'emissivity' is used to characterize the efficiency of a surface to emit infrared radiation, compared to a black body source. Accurate emissivity mapping is crucial to enable the actual surface temperature of the powered device to be obtained.

3.2 Experiment Parameters:

The semiconductor device under test was a 2x150 μm wide, 0.25 μm long AlGaN/GaN HEMT with 3 μm source/drain spacing and the following epi-layer structure: 10 nm of InAl(Ga)N with a 1 nm AlN interlayer on a 50 nm GaN channel, a 1.5 μm AlGaN buffer (5% Al) and a 100 nm AlN nucleation layer on a thinned SI SiC substrate. Thermal maps were recorded using a Quantum Focus Instrument (QFI), IR thermal imager with bias conditions of V_{ds}= 7 V. The device was operated with the heated base plate set to 85 °C to provide a uniform thermal background for IR imaging. A long gate AlGaN/GaN HEMT with gate length 20 μm, width W_g = 300 μm and 5 μm source/drain spacing, was also used for hall effect measurement of 2DEG carrier density (n_s) and electron mobility (μ_n) verses gate bias, where temperature dependent low field 2DEG mobility's were extracted on a 40 x 400 μm ungated AlGaN/GaN HEMT.

4. ALGAN/GAN HEMT THERMAL ANALYSIS

DC electrical techniques are obviously the simplest and cheapest, since they are often relying only on standard I–V measurements at different ambient temperatures. The main drawback with respect to pulsed methods is the need to rely sometimes on drastic simplifying assumptions [13], including the independence of the thermal resistance with temperature and dissipated power. The method assumes a linear dependence of the drain current (I_D) on the channel temperature once the linear dependence of I_D on the ambient temperature (T_A) has been experimentally demonstrated. It therefore relies on the choice of suitably narrow intervals of T_A and dissipated power (PD), wherein the drain–current temperature dependence can be linearized with good accuracy and R_{TH} can be considered constant; apart from this, no other simplifying assumption is necessary.

4.1 Temperature Effect on AlGaN/GaN HEMT:

(i) The effects of temperature on HEMT performance include variations in transconductance, input capacitance, and device resistance.

(ii) Transconductance variations are caused by an increase in electron mobility in the active channel as the temperature decreases.

(iii) Variation of input capacitance is induced by an increase in the built-in Schottky voltage as temperature decreases.

5. ALGAN/GAN HEMT: ANALYTICAL MODELING

In order to obtain an analytical expression for the saturation current I_{dsat} we need the velocity-field relationship. Many theoretical works predicted for bulk GaN material the existence of a peak velocity of 3 x 10^7 cm/s for a range of electric fields between 100 to 200 kV/cm and a saturation around 2 x 10^7 cm/s at higher fields. Although theoretical works predicted also velocity overshoot for 2DEG in AlGaN/GaN heterostructures, it is not obvious that these results are in agreement with the real world. Different differential equations have material-specific parameters, such as band gap energy, electron mobility, thermal conductivity, etc. The dependence of these parameters on temperature, energy, etc. is described by models, which are presented in the following.

5.1 Band gap energy: Temperature dependence of the band gap in nitrides is calculated by:

$$E_g = E_{g,0} - \frac{\alpha_g T_L^2}{\beta_g + T_L}$$

$E_{g,0}$ = energy band gap at 0 K, For calculations we

(1)Where

considered $E_{g,0}$ = 3.4 eV. α_g and β_g are empirical constants for GaN. In case of GaN the value of α_g = 9.09 x 10^{-4} eV/K and β_g = 800 K has been taken for the calculations. The parameter values for GaN are an average of various reported results as summarized in [14] while those for AlN are based on the experimental work of Guo et al. 1994 [15]. In case of

AlN the value of $E_{g,0}$ = 6.2 eV, α_g = 18.0 x 10^{-4} eV/K and β_g = 1462 K has been taken for the calculations. The band gap of AlGaN then evaluated as given below:

$$E_g^{AlGaN} = E_g^{AlN}(1-\chi) + E_g^{GaN}\chi + C_g(1-\chi)\chi$$

(2)Where, the values of C_g has been taken as zero, which show the linear variation and for χ = 0.22, the valance band offset agains GaN is 0.25. In eq. (2) the different material different valance band, which are aligned by applying correction factor, known as energy offset (E_{off}). The energy offset has been calculated for AlGaN as presented below:

$$E_{off}^{AlGaN} = \frac{E_{off}^{AlN}(E_g^{AlGaN} - E_g^{GaN}) - E_{off}^{GaN}(E_g^{AlGaN} - E_g^{AlN})}{E_g^{AlN} - E_g^{GaN}}$$

(3)Where the energy offset (E_{off}) for GaN and AlN are represented by E_{off}^{GaN} and E_{off}^{AlN} respectively. The energy offset (E_{off}) for GaN is set 0 eV because valance band of GaN has been taken as reference and the energy offset (E_{off}) for AlN was taken as 1.2 eV as reported in literature. We have determined the barrier height of the Schottky contact to GaN to be 1.0 eV at room temperature which is compared and contrasted with simulated and experimentally evaluated data by our group provided good agreement. The changes in the barrier height with temperature have been observed by different simulated results.

5.2 Thermal conductivity: For AlGaN/GaN HEMT the thermal conductivity is modeled by a power law, which is given as below:

$$k(T_L) = k_{300}\left(\frac{T_L}{300K}\right)^{\alpha} \quad (4)$$

where k_{300} is the value at 300 K. The value of k_{300} = 130 W/mK for 'bulk' GaN, which was extracted from early experiments data reported. The parameter α, which are models the decrease with temperature. At k_{300} = 130 W/mK; α = -0.43.

5.3 Mobility model: Over the years the electron mobilities increase due to the improved quality of the material samples. The electron mobility as a function of temperature in the two-dimensional electron gas (2DEG) as experimentally determined by various groups. The 2DEG mobility exhibits overall higher values especially at high temperatures, while retaining the trend for improved results over time. The low-field mobility is modeled by an expression similar to that proposed by Caughey and Thomas [4, 16, 17].

$$\mu^{LI} = \mu^{\min} + \frac{\mu^L - \mu^{\min}}{1 + \left(\frac{C_I}{C^{ref}}\right)^{\gamma_0}} \quad (5)$$

Where, C_I denotes the concentration of ionized impurities, μ^L is the mobility in undoped material, μ^{min} is the mobility in highly doped material, limited by impurity scattering.

In order to model the temperature dependence the mobilities are additionally evaluated using power laws, which is presented as following:

$$\mu^L = \mu_{300}^L + \left(\frac{T_L}{300K}\right)^{\gamma_1} \quad (6)$$

$$\mu^{\min} = \mu_{300}^{\min} + \left(\frac{T_L}{300K}\right)^{\gamma_2} \quad (7)$$

These type of similar expressions have been used also by other authors in reported literatures. To evaluate the values of γ_1 and γ_2 parameters the Monte Carlo simulations have been carried out and the electron mobility variation in AlGaN/GaN HEMT with temperature has been also presented in the result and discussion section.

5.4 Thermal Resistance Measurement:

The drain current I_D, at a fixed value of the gate–source voltage V_{GS0} and for a drain–source voltage V_{DS} biasing the HEMT in saturation, is analytically observed to be a linear function of T_A, i.e.,

$$I_D\left(V_{GS0}, V_{DS}, T_A\right) = I_D\left(V_{GS0}, V_{DS}, T_{A0}\right) + h.\left(T_A - T_{A0}\right) = I_{D0} + h.\left(T_A - T_{A0}\right) \quad (8)$$

where T_{A0} is a reference ambient temperature, h can be measured by plotting I_D versus T_A and interpolating with a straight line. If it exists, the observed linear dependence (8) must be due to a linear dependence of I_D on T_C

$$I_D\left(V_{GS0}, V_{DS}, T_C\right) = I_{D0} + h.\left(T_C - T_{C0}\right) \quad (9)$$

where T_{C0} is the channel temperature determined by T_{A0}, V_{GS0}, and V_{DS}. This is given by definition of the thermal resistance R_{TH} as presented below:

$$T_C - T_{C0} = T_A - T_{A0} + R_{TH}.V_{DS}.\left(I_D - I_{D0}\right) \quad (10)$$

By substituting eq. (10) into eq (9) and rearranging the equation, we obtains the final expression as given below:

$$\frac{1}{h} = \frac{1}{h'} - R_{TH}.V_{DS} \quad (11)$$

This procedure repeated at different values of V_{DS} in the saturation region and 1/h can be plotted versus V_{DS}. If the model is correct, the plot should be a straight line based on eq (11), and R_{TH} can be obtained as the slope of the best fit line. The result obtained has be shown in the result and

discussion section which is compared and contrasted with the reported data for the validity of the model.

6. RESULTS AND DISCUSSIONS:

The thermal measurement using an IR thermal microscope facility has been established, employing a Quantum Focus Instrument (QFI) and analytical modeling using simulation scheme has been presented for AlGan/GaN HEMT. For the purpose of validation of measurements, an analytical modeling and simulation approach, the results obtained has been compared and contrasted with reported simulated results as well as experimental results. The typical current voltage out characteristics of GaN HEMT has been shown in the figure 3. The variation of drain current with applied drain to source voltage (V_{DS}) for measured data, simulated result, experimental data, and reported result are presented. This result reveals a good agreement of output characteristics for experimental data, reported simulated result and measured data in linear region instead of saturation region, by the use of improved model, which validate our approach.

In figure 4 out characteristics showing the variation of drain current with applied drain to source voltage of AlGaN/GaN HEMT for different values of gate voltage at T = 425 K and L_g = 0.25 µm. The gate voltage has been varied from 0 V to + 2V in intervals and the simulated out characteristics has been observed same as for the reported HEMT device. There is slightly different found in measured and simulated data. In saturation region the measured data decreased, this is due to the fact of internal heating of the measuring instrument. The variation drain current with drain voltage at channel length of L_g = 0.25 µm, L_g = 0.5 µm, L_g = 0.75 µm for AlGaN/GaN HEMT device has been shown in figure 5 for both measured and simulated result. It can be seen from the figure that as we downscale the HEMT device from L_g = 0.75 µm to L_g = 0.25 µm the drain current increased, hence the driving capability enhanced with down scaling the HEMT device, which is true for the Si devices also. This can be attributed to the fact that as the channel length (L_g) reduces the longitudinal electric field enhances, thereby increasing the drain current. It is again noted that the measured data have more accurate matching in linear region as compared to the saturation region.

Figure 6 shows the I-V transfer characteristics of drain current with applied gate voltage at channel length of L_g = 0.25 µm, L_g = 0.5 µm, L_g = 0.75 µm for HEMT device for measured and simulated data. From the figure it can be inferred that in the subthreshold operation drain current drastically reduces with the reduction in gate voltage as is true for bulk semiconductor devices as well. In this case the measured data recorded is lower than that of simulated data. This is due to the internal resistance of device under the influence of applied gate voltage. In Figure 7, I-V transfer characteristics showing the Variation of drain current with applied gate voltage for different temperature of 300 K, 365 K, 425 K and 500 K. It is observed from the result that as the temperature increased for any fixed value of gate voltage the drain current decreases. This is due to the fact that, with increase in temperature the charge carriers start moving in zigzag motion and due to collision the effective drain current decreases.

Variation of drain current with temperature for different values of drain voltage is shown in figure 8. It can be seen from the figure that for any fixed value of drain source voltage (V_{DS}) the drain current decreases with increase in temperature and at the same time for a constant temperature the drain current increase with decrease in the applied drain source voltage. The temperature increase is observed already at low drain voltages, especially at high gate voltages. Hence, implementation of self heating effect is necessary step toward characterization of high power and high temperature HEMT devices. In Figure 9 variation of electron mobility in GaN with temperature for reported result and proposed model of HEMT has been shown. It is seen that the proposed HEMT model is more robust to the temperature variation that the reported Schwierz-2005 model and have higher electron mobility. The variation of electron mobility with temperature at AlGaN/GaN interface is shown in figure 10. For the purpose of validation the results obtained through our model has been compared and contrasted with reported Huque-2009 model.

7. CONCLUSION

This paper deals with measurements and analytical modeling of AlGaN/GaN HEMT. Temperature profiles were measured on the operating AlGaN/GaN HEMT device using Quantum Focus Instrument (QFI), IR thermal imaging spectroscopies. Using an accurate modeling process and measurement techniques, an optimized AlGaN/GaN structure has been designed for high power and high frequency applications. Analytical modelling and simulations of GaN HEMT structure has been carried out to evaluate band gap energy, thermal conductivity, electron mobility and the various characterizes. Furthermore, simulations were compared to electrical measurements and reported results for validation purpose. A strong attention must be paid to thermal management. A wide range of techniques exist for performing temperature measurements on semiconductor devices, while Infrared thermal microscopy used to rapidly obtain two-dimensional temperature measurements on structures such as HEMTs.

8. REFERENCES

[1] M.J. Rosker, “The present state of the art of wide-bandgap semiconductors and their future,” Radio Frequency Integrated Circuits Symposium, IEEE, pp. 159–162, June 2007.

[2] K. Krishnamurthy, J. Martin, B. Landberg, R. Vetury, M.J. Poulton, “Wideband 400W pulsed power GaN HEMT amplifiers,” Microwave Symposium Digest, IEEE MTT-s Int, pp. 303–306, June 2008.

[3] S. Vitanov, V. Palankovski, S. Maroldt, R. Quay, “High-temperature modeling of AlGaN/GaN HEMTs” , Solid-State Electronics, vol. 54, pp. 1105–1112, 2010.

[4] D. Francis, J. Wasserbauer, F. Faili, D. Babić, F. Ejeckam, W. Hong, P. Specht, E.R. Weber, “GaN HEMT Epilayers on Diamond Substrates” , Proceeding CS MANTECH, Austin, TX, pp. 14–17, May, 2007.

[5] Roberto Menozzi, Gilberto A. Umana-Membreno, Brett D. Nener, Giacinta Parish, Giovanna Sozzi, Lorenzo Faraone and Umesh K. Mishra, “Temperature-Dependent Characterization of AlGaN/GaN HEMTs: Thermal and Source/Drain Resistances” , IEEE Transactions on Device and Materials Reliability, vol. 8, no. 2, pp. 255-264, 2008.

[6] E. R. Heller and A. Crespo, “Electro-thermal modeling of multifinger AlGaN/GaN HEMT device operation including thermal substrate effects.”, Microelectron. Reliab. Vol. 48, pp. 45- 50, 2008.

[7] E. R. Heller, "Simulation of Life Testing Procedures for Estimating Long-Term Degradation and Lifetime of AlGaN/GaN HEMTs", IEEE Transactions on Electron Devices, vol 55, pp. 2554-2560, 2008.

[8] A. Sarua, H. Ji, M. Kuball, M. J. Uren, T. Martin, K. P. Hilton, and R. S. Balmer, "Integrated micro-Raman/infrared thermography probe for monitoring of self-heating in AlGaN/GaN transistor structures", IEEE Trans. Electron Devices, vol. 53, issue 10, pp. 2438-2447, 2006.

[9] M. Kuball, J. M. Hayes, M. J. Uren, T. Martin, J. C. H. Birbeck, R. S. Balmer, and B. T. Hughes, "Measurement of temperature in active high-power AlGaN/GaN HFETs using Raman spectroscopy", IEEE Electron Device Lett., vol. 23, issue 1, pp. 7-9, 2002.

[10] N. Shigekawa, K. Onodera, and K. Shiojima, "Device Temperature Measurement of Highly Biased AlGaN/GaN High-Electron-Mobility Transistors", Jpn. J. Appl. Phys. Vol. 42, no. 4B, pp. 2245-2249 (2003).

[11] H. Kroemer, Wu-Yi Chien, J. S. Harris and D. D. Edwall, "Measurement of isotype heterojunction barriers by C-V profiling," Appl. Phys. Lett. vol. 36, pp. 295, 1980.

[12] M. Kuball, S. Rajasingam, A. Sarua, M. J. Uren, T. Martin, B. T. Hughes, K. P. Hilton, and R. S. Balmer, "Measurement of temperature distribution in multifinger AlGaN/GaN heterostructure field-effect transistors using micro-Raman spectroscopy" , Appl. Phys. Lett., vol. 82, no. 1, pp. 124– 126, Jan. 2003.

[13] J. Kuzmík, P. Javorka, A. Alam, M. Marso, M. Heuken, and P. Kordos, "Determination of channel temperature in AlGaN/GaN HEMTs grown on sapphire and silicon substrates using DC characterization method" , IEEE Trans. Electron Devices, vol. 49, no. 8, pp. 1496–1498, Aug. 2002.

[14] I. Vurgaftman, J. Meyer, Ram Mohan, "Band parameters for III–V compound semiconductors and their alloys" , J Appl Phys, vol. 89, issue 11, pp. 5815–5875, 2001.

[15] Q. Guo, A. Yoshida, "Temperature dependence of band gap change in InN and AlN" , Jpn J Appl Phys, vol. 33, issue 5A, pp. 2453–2456, 1994.

[16] D. Caughey, R. Thomas, "Carrier mobilities in silicon empirically related to doping and field" , Proceeding IEEE, vol. 55, issue 12, pp. 2192–2193, 1967.

[17] V. Palankovski, R. Quay, "Analysis and simulation of heterostructure devices" , Wien/New York: Springer; 2004.

[18] J. Michael Golio, Eric N. Arnold, andWilliam B. Beckwith, Microwave MESFETs and HEMTs, Artech House London (1991).

[19] B. Gil, Group III Nitride Semiconductor Compounds, Physics and Applications, Clarendon Press, Oxford (1998.

[20] Mehrotra, Vivek, Boutros, Karim, Brar and Berinder, "Electric-Field Dependence of Junction Temperature in GaN HEMTs," Device Research Conference, 2007 65th Annual , pp.143-144, 18-20th June 2007.

[21] Raphal Aubry, Jean-Claude Jacquet, J. Weaver, Olivier Durand, P. Dobson, G. Mills, Marie-Antoinette di Forte-Poisson, Simone Cassette and Sylvain-Laurent Delage, "SThM Temperature Mapping and Nonlinear Thermal Resistance Evolution With Bias on AlGaN/GaN HEMT Devices," Electron Devices, IEEE Transactions on , vol. 54, no. 3, pp.385-390, March 2007

[22] C. H. Oxley, B. M. Coaker, and N. E. Priestley, .Measured thermal images of a gallium arsenide power MMIC with and without RF applied to the input,. Solid-State Electronics, vol. 47, no. 4, pp. 755-758, April 2003

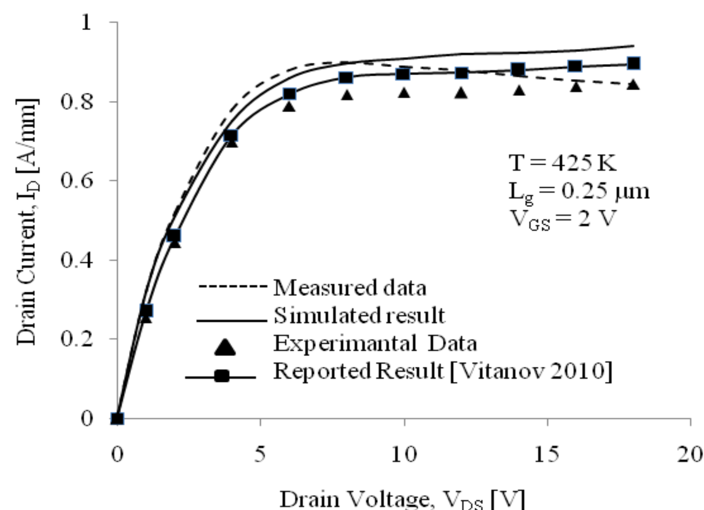

Figure 3: GaN HEMT's out characteristics for measured data, simulated result, experimental data, and reported result

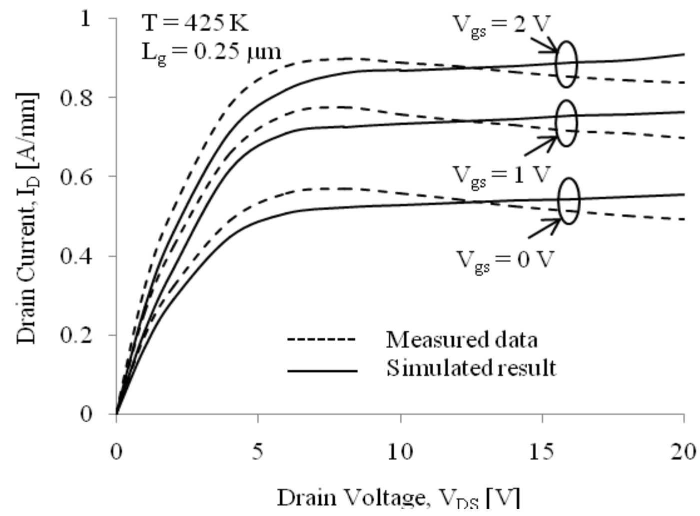

Figure 4: GaN HEMT's out characteristics for gate voltage of 0V, 1V, 2V at T = 425 K and L_g = 0.25 µm.

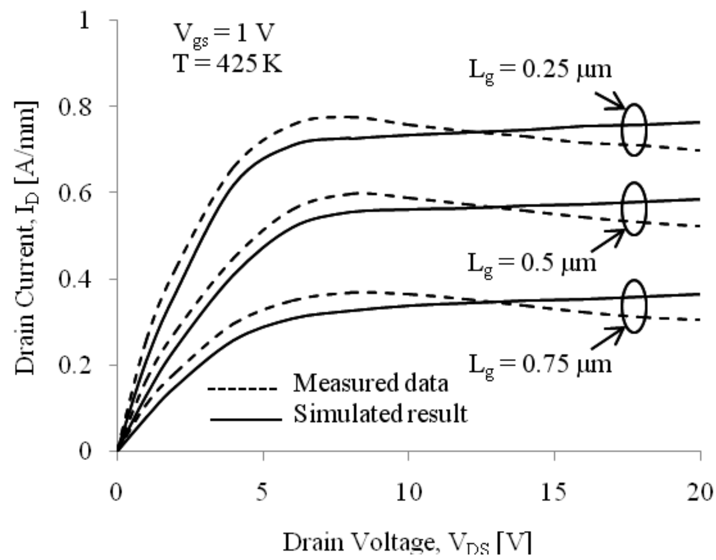

Figure 5: Variation drain current with drain voltage for measured data and simulated result at different channel length of GaN HEMT device

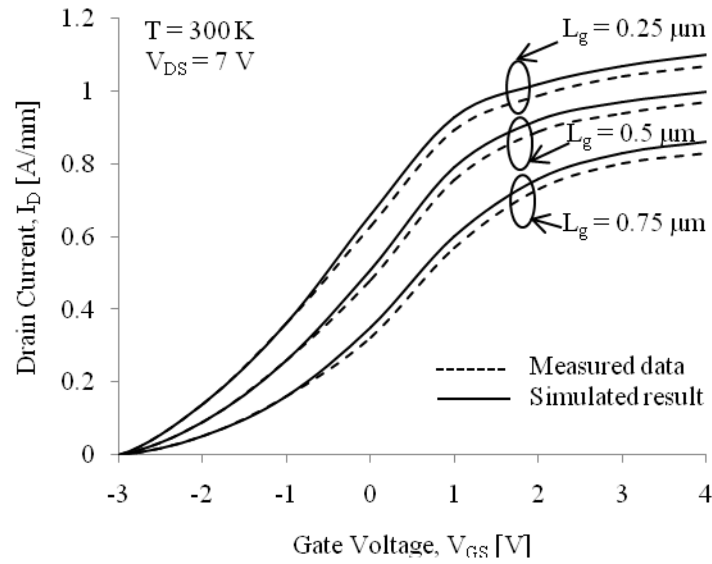

Figure 6: I-V transfer characteristics showing the variation of drain current with applied gate voltage for measured data and simulated result at different channel length of GaN HEMT device

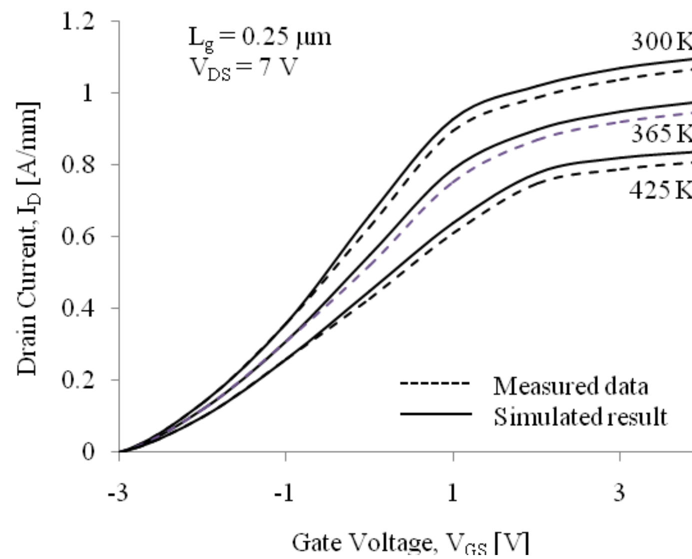

Figure 7: I-V transfer characteristics showing the Variation of drain current with applied gate voltage of measured data and simulated result for different temperature

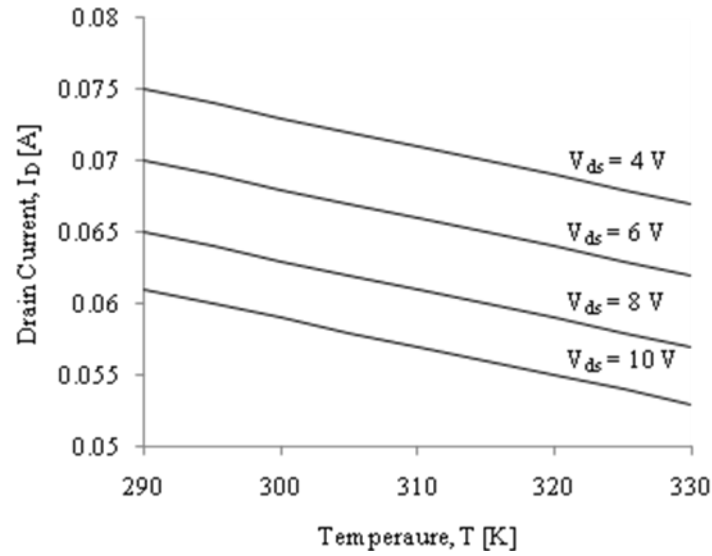

Figure 8: Variation of drain current with temperature for different values of drain voltage

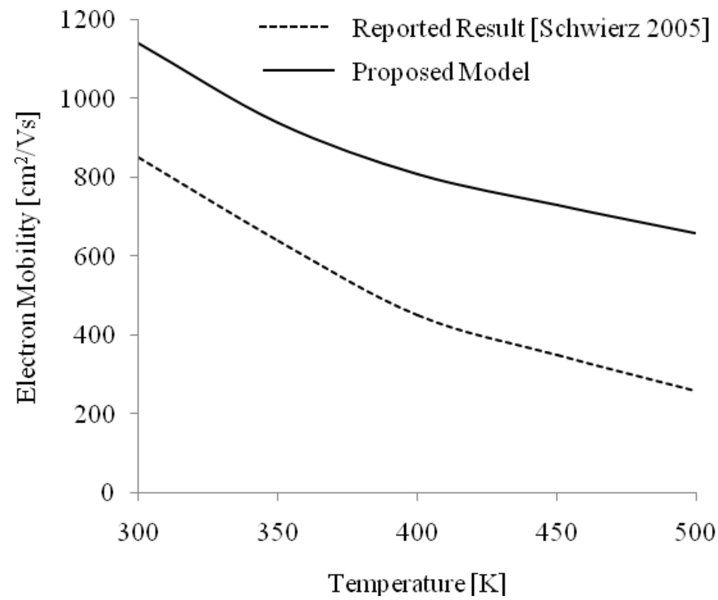

Figure 9: Variation of electron mobility in GaN with temperature for reported result and proposed model of HEMT

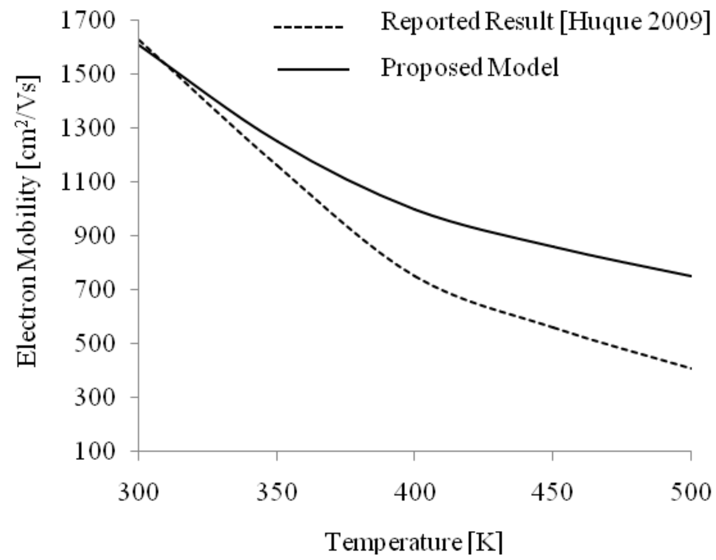

Figure 10: Variation of electron mobility with temperature at AlGaN/GaN interface